The Joint Use of Catastrophe Theory and Electron Localization Function to Characterize Molecular Mechanisms. A Density Functional Study of the Diels−Alder Reaction between Ethylene and 1,3-Butadiene

Slawomir Berski,[†,‡] Juan Andrés,[*,†] Bernard Silvi,[§] and Luis R. Domingo[||]

Departament de Ciències Experimentals, Universitat Jaume I, Apartat 224, 12080, Castelló, Spain, Laboratoire de Chimie Théorique, Université Pierre et Marie Curie, 4 Place Jussieu, 75252 Paris Cedex, France, and Departamento de Química Orgánica, Instituto de Ciencia Molecular, Universidad de Valencia, Dr. Moliner 50, 46100 Burjassot, Valencia, Spain

Received: February 27, 2003; In Final Form: May 20, 2003

The catastrophe theory has been used to investigate the reorganization of the localization basins, within the electron localization function formalism, along the intrinsic reaction coordinate associated with the reaction pathway of the Diels−Alder reaction between ethylene and 1,3-butadiene. There are distinguished seven phases (I−VII) characterized by a decay and formation of the double bonds, an accumulation of the nonbonding electron density on the C atoms involved in the formation of two sigma bonds and a ring closure processes. During the reaction 10 catastrophes occur belonging to two elementary types: fold and cusp. The transition structure is located in phase III, being determined by a "reduction" of the double C═C bond of ethylene to the single bond, and it is not associated with any special event on the intrinsic reaction coordinate path. For the first time, it is shown that formation of two new sigma C−C bonds between ethylene and 1,3-butadiene begins in phase VI at 2.044Å.

1. Introduction

Determination of reaction mechanism for a given chemical rearrangement is an issue of major concern in chemistry. The classical approaches toward the quantum mechanical representation of chemical reactions are based in the evolution of energy and charge redistribution along the channel connecting the reactants to products. In the first case, the potential energy profile associated with the reaction pathway connecting the stationary points—reactants, products, possible intermediates, and transition structures—is obtained. By means of the characterization of these stationary points on the potential energy surface for a similar set of reactions, chemical reactivity trends can be deduced. In the second method, a chemical reaction can be seen as resulting from redistribution of electron density along the reaction pathway connecting these stationary points. This density rearrangement takes place among the atoms defining the reactive system, being the total number of electrons conserved throughout the process. However, how the first energy-based method is related to charge redistribution accompanying the bond breaking/forming processes the reaction pathway remains unclear. A better mechanistic understanding of how bond breaking/forming processes take place will facilitate progress in this area. Although the use of these standard methods is instructive and efficient to the discussion of reaction mechanism, theoretical analysis should be performed to correlate with quantum mechanical concepts derived from first principle calculations.

In recent years, two procedures have been proposed to obtain a robust quantitative definition of chemical bonding. The delocalization index[1−3] based on the electron pair density in the atoms in molecules AIM approach of Bader[4] and a bond basin populations from the electron localization function (ELF) approach of Becke and Edgecombe[5] as extensively developed by Silvi and Savin.[6−12] In particular, ELF approach is topological and divides a system's space into basin attractors based on the gradients of particular scalar fields. ELF basins are defined quantities, although based on strong physical arguments regarding the Fermi hole[13,14] that can be interpreted consistently on the simple ideas of chemical bonding associated to the Pauli exclusion principle. A wide range of applications of the ELF method for the treatment of chemical reactivity has also appeared.[15−29]

Applications of singularity theory to the study of bifurcations of equilibrium states in the theory of different physical processes are well-founded.[30] Krokidis and Silvi proposed a joint use of the ELF approach and the catastrophe theory[31,32] (bond evolution theory (BET)) to identify changes between regions of structural stability in processes of breaking of the ethane C−C, the dative bond in H_3NBH_3, and ammonia inversion.[32] It has been also applied to important chemical reactions such as proton transfers,[33,34] electron transfer,[35] isomerization,[36] and transition metal intercalation.[37] Following those proposals, we extent the study to the prototype of a pericyclic concerted Diels−Alder (DA) reaction with the aim of examining the usefulness of this theoretical analysis in the context of electron reorganization and chemical reactivity of molecular reaction.

The DA reaction has become one of the most widely used methods in synthetic organic chemistry for carbon−carbon bond formation and has been central in the developments of theoretical models of pericyclic reactions.[38,39] Not surprisingly, considerable attention has been paid to the elucidation of its molecular

* Corresponding author. E-mail: andres@exp.uji.es.
[†] Universitat Jaume I.
[‡] Permanent affiliation: Faculty of Chemistry, University of Wroclaw, F. Joliot-Curie 14, 50−383 Wroclaw, Poland.
[§] Université Pierre et Marie Curie.
[||] Universidad de Valencia.

10.1021/jp030272z CCC: $25.00
Published on Web 07/10/2003

mechanism.[40,41] In particular, the DA reaction between ethylene and 1,3-butadiene to yield cyclohexadiene is often taken as the classical example of a pericyclic reaction.[41,42] Despite of its seeming simplicity, the nature of the reaction mechanism was not free from controversy, and it has been the subject of numerous experimental and theoretical studies.[43−48] The Woodward−Hoffmann selection rules for [4+2] pericyclic cycloaddition rearrangements and the analysis of potential energy surface, based on ab initio density functional theory (DFT) and CASSCF and CAS-MP2 calculations, renders that the preferred reactive channel takes place along a concerted six membered transition structure (TS),[43,47] although a stepwise mechanism involving the formation of intermediates can coexist.[47,49]

The layout of this paper is as follows: section 2 is devoted to a description of the topological analysis of the electron localization function and principles of the catastrophe theory, methods adopted in this paper, section 3 presents details of the computational procedures, and section 4 reports results and discussion. A short section of conclusions closes the paper.

2. Method of Analysis

Our goal is to characterize the bonding and its evolution along the reaction path in terms of simple chemical concepts such as bonds and lone pairs. The topological analysis of the electron localization function ELF[5−6,28] provides a mathematical model of the Lewis's valence theory[50,51] since it yields a partition of the molecular position space into basins of attractors presenting a one-to-one correspondence with the expected chemical objects. It is rooted on the chemical meaning of the function for which several interpretations have been proposed.[5,7,52,53] The ELF function was designed by Becke and Edgecombe[5] to provide an orbital independent description of the electron localization. The expression for ELF is

$$\eta(\mathbf{r}) = \frac{1}{1 + \left(\frac{D_\sigma}{D_\sigma^0}\right)^2} \tag{1}$$

in which D_σ and D_σ^0 represent the curvature of the electron pair density for electrons of identical σ spins (Fermi hole) for, respectively, the actual system and a homogeneous electron gas with the same density. The analytical form of ELF confines its value between 0 and 1. The original derivation of the ELF function considers the laplacian of the Hartrre−Fock conditional probability of finding a σ-spin electron at position when a first electron is located at $\mathbf{r}_1$

$$D_\sigma = (\nabla_2^2 P_{\mathrm{cond}}^{\sigma\sigma}(1,2))_{1=2} = \sum_{i=1}^{i=N} |\nabla\varphi_i|^2 - \frac{1}{4}\frac{|\nabla\rho^\sigma(1)|^2}{\rho^\sigma(1)} \tag{2}$$

The D_σ has the significance of the local excess of kinetic energy due to the Pauli repulsion. In regions of space dominated by an antiparallel spin pair character, the Pauli repulsion is weak, and therefore, ELF is close to 1. Near the boundary between two such regions, where some spin electrons necessarily come close together, they exert a significant Pauli repulsion which decreases the value of the ELF function to low values.

It can be shown that the ELF formula is a very good approximation of the normalized spin pair composition.[52] The spin pair composition at position $\mathbf{r}$ is defined as

$$c_\pi^0(\mathbf{r}) = \bar{N}_V^{-2/3}(\mathbf{r})\frac{\bar{N}_{||}(\mathbf{r};V)}{\bar{N}_\perp^0(\mathbf{r};V)} \tag{3}$$

where V is an arbitrary volume around the reference point, $\bar{N}_V(\mathbf{r})$ the integrated density over this volume, $\bar{N}_{||}(\mathbf{r};V)$ the same spin pair population within V, and $\bar{N}_\perp^0(\mathbf{r};V)$ the independent particle closed shell and antiparallel pair population of V for the same local total density $\rho(\mathbf{r})$. For $\bar{N}_V(\mathbf{r}) \leq 10^{-3}$, $c_\pi^0(\mathbf{r})$ is independent of $\bar{N}_V(\mathbf{r})$; it tends to zero either for perfect antiparallel pairing (i.e., a localized Lewis pair) or for single electron localization in the case of radicals.

The *ELF* function, $\eta(\mathbf{r})$, depends on parameters such as the nuclear coordinates of the system, its electronic state, etc., which constitute the control space $\{\alpha\}$. The gradient dynamical system of ELF is characterized by its critical points at position $\mathbf{r}_C$, that is the points at which

$$\nabla\eta(\mathbf{r}_C;\{\alpha\}) = 0 \tag{4}$$

The number of positive eigenvalues of the Hessian (second derivatives) matrix at $\mathbf{r}_C$ is called the index of the critical point denoted $I(P)$. In $\mathbf{R}^3$, $I(P)$ ranges from 0 to 3. The local maxima are critical points with $I(P) = 0$ and are named attractors. The stable manifold, i.e., the set of points defining all the trajectories ending at a given critical point, of an attractor is named a basin. The separatrices, which are the bounding surfaces, lines, and single points between basins, are the stable manifolds of critical points having at least one strictly positive index. These topological concepts are closely related to those of river basins and watersheds used in geography. There are basically two kinds of basins: on one hand are the core basins, C(A), encompassing the nuclei with $Z > 2$ and of atomic symbol A, and on the other hand the valence basins, V(A, B, ...), the union of which constitute the valence shell of the molecule. The valence basins are characterized by their synaptic order, which is the number of core basins with which common boundary is shared.[8] When proton is located within a valence basin, it is counted as formal core. Monosynaptic basins are associated to lone pairs and disynaptic ones to two center bonds, whereas polysynptic basins are the signature of multicentric bonds. Quantitatively, basin properties are calculated by integrating the relevant density of property, e.g., the basin population, which can be written as the sum of its spin contributions in the case of open shell systems:

$$\bar{N}(\Omega_i) = \int_{\Omega_i} \rho(\mathbf{r})\, \mathrm{d}\mathbf{r} = \bar{N}^\alpha(\Omega_i) + \bar{N}^\beta(\Omega_i) \tag{5}$$

It is worthy to calculate the variance of the basin population:

$$\sigma^2(\bar{N};\Omega_i) = \int_{\Omega_i} \mathrm{d}\mathbf{r}_1 \int_{\Omega_i} \pi(\mathbf{r}_1,\mathbf{r}_2)\, \mathrm{d}\mathbf{r}_2 - [\bar{N}(\Omega_i)]^2 + \bar{N}(\Omega_i) \tag{6}$$

where $\pi(\mathbf{r}_1,\mathbf{r}_2)$ is the spinless pair function. The variance is a measure of the quantum mechanical uncertainity of the basin population, which can be interpreted as a consequence of the electron delocalization. The relative fluctuation of the basin population

$$\lambda(\bar{N};\Omega_i) = \frac{\sigma^2(\bar{N},\Omega_i)}{\bar{N}(\Omega_i)} \tag{7}$$

provides an additional indication of the delocalization within the Ω_i basin. Another important concept is that of domain initially introduced by Mezey.[54] An f-localization domain is a volume bounded by the isosurface $\eta(\mathbf{r}) = f$. It is said to be irreducible if it contains one and only one attractor, reducible otherwise.

A fundamental concept of mathematical theory of dynamical systems is the structural stability. A dynamical system is said structurally stable if a small perturbation of the vector field does not change the indexes of its critical points. A gradient dynamical system is structurally stable if all its critical points are hyperbolic (i.e., all of the Hessian matrix eigenvalue are different of zero) and if there is no saddle connections (i.e., trajectories joining saddle points). The number of critical points satisfies the Poincaré−Hopf formula:

$$\sum_{P}(-1)^{I(P)} = \chi(M) \tag{8}$$

in which the sum is performed over the critical points, $I(P)$ is the index of the critical point labeled by P and $\chi(M)$ is the Euler characteristic of the manifold on which the gradient field is bound, i.e., 1 for a molecule, 0 for a periodic system.

In our mathematical model, a chemical reactive process corresponds to changes of the number and types of the critical points of the dynamical systems occurring when the control space parameters evolve from the initial subset of values of the reactives $\{\alpha_I\}$ to the final subset of the products $\{\alpha_F\}$. Since the critical points always obey the Poincaré−Hopf formula, this latter appears to be a very strong constraint ruling the chemical mechanisms. The control space can be considered as the union of subsets within which all the critical points remain hyperbolic, the structural stability domains and those which correspond to given chemical structures. At the turning points between these domains, at least one critical point becomes nonhyperbolic, enabling its index to change. Such a discontinuity is called a bifurcation catastrophe. The behavior of dynamical systems upon bifurcations constitute an important part of René Thom's catastrophe theory.[31] According to this theory, there are seven types of elementary catastrophes, which have been classified by Thom according to their universal unfolding. The universal unfolding of a catastrophe is a simple parametric polynomial function of degree higher than 2, which models the local behavior of the dynamical system upon a change of the control space parameters. The number of parameters involved in the unfolding expression is the dimension of the active control space. The catastrophe theory has been applied to the study of the gradient vector fields of the electron density and of the ELF function. The electron density enables investigating the structural evolution occurring in cases such as isomerization,[55] ring and cage formations,[56] and exceptional situations characterized by non-nuclear attractors,[57] but it is unable to evidence any topological change for important phenomena such as the formation of a covalent bond. The BET developed by Krokidis et al.,[32] which applies the catastrophe theory to the ELF gradient field, overcome this difficulty. It classifies the elementary chemical processes according to the variation of either the number of basins, the morphic number μ, or the synaptic order σ of at least one basin. There are accordingly three type of chemical processes which correspond to $\Delta\mu > 0$, $\Delta\mu < 0$ and $\Delta\mu = 0$, $\Delta\sigma \neq 0$.

Only three elementary catastrophes have been recognized so far in the chemical reactions: the fold, cusp, and elliptic umbilic catastrophe. The fold catastrophe transforms a wandering point (i.e., a point which is not a critical one) into two critical points of different parity. Its unfolding is $x^3 + ux$: x is the direction of the eigenvector corresponding to the eigenvalue of the Hessian matrix which changes of sign, and u is the control space parameters which governs the discontinuity. For $u > 0$, the first derivative is positive for all x, the catastrophe takes place at $u = 0$, for which both first and second derivatives are zero, and for $u < 0$ there are two critical points at $x = \pm\sqrt{u/3}$. The cusp catastrophe transforms a critical point of a given parity into two critical points of the same parity and one of the opposite parity. Finally, the elliptic umbilic catastrophe changes the index of one critical point by 2.

3. Computational Methods

The calculations have been performed by means of the density functional theory using the B3LYP functional[58−60] with the 6-31G(d) basis set as included in Gaussian 98 program.[61] Harmonic vibrational frequency calculations were carried out for the stationary points to confirm each structure being either a minimum, with no imaginary frequency, or a transition structure (TS), with one imaginary frequency. The reaction path has been followed using the intrinsic reaction coordinate (IRC) method[62,63] in mass-weighted internal coordinates going in the forward and reverse directions from TS. A number of 102 points has been used with the step size equaled to 0.01 amu$^{1/2}$bohr. It corresponds to a beginning location of ethylene and 1,3-butadiene at the $R(C_1\cdots C_6)$ and $R(C_4\cdots C_5)$ distances of 2.85 Å and final of 1.549 Å, which has been identified as the minimum on the potential side. In the text below, the phrase "the reaction path" corresponds to a fragment of the reaction path as explained above. The topological analysis of ELF has been carried out by the TopMod program[64] and graphical representation by SciAn.[65] The ELF function has been calculated over a rectangular parallelepipedic grid with step size smaller than 0.1 bohr. The properties of critical points have been analyzed using the top_search program within the TopMod suit. A critical distance at which a catastrophe occurs is denoted as R_C and it corresponds to the $R(C_1\cdots C_6)$ and $R(C_4\cdots C_5)$ distances between reacting molecules.

4. Results and Discussion

4.1. A Topological Analysis of the ELF Function. There are distinguished seven phases (I−VII) characterized by a decay and formation of the double bonds, an accumulation of the nonbonding electron density on the C atoms involved in the formation of two sigma bonds and a ring closure processes. During the reaction 10 catastrophes occur belonging to two elementary types: fold and cusp.

Phase I of the reaction starts for isolated ethylene and 1,3-butadiene molecules. The graphical representation of localization basins in both molecules and they mutual orientation during the reaction course may be deduced from Figure 1 where the transition state is presented. In 1,3-butadiene there are found four core basins of carbon $C(C_{i=1,4})$ which characterize the electron density of core regions. Their basin populations ($\bar{N}$) amount to 2.06e. Six carbon−hydrogen bonds are represented by protonated disynaptic basins $V(H_{j=1,6},C_{i=1,4})$ with values of $\bar{N}$ equal to 2.10 and 2.09 e for terminal C−H bonds and 2.10 e for C_2-H_3 and C_3-H_4. In the case of C−C bonds the ELF method yields an essential differentiation between the single and double bonds being in accordance to the classical Lewis representation. The double $C_1{=}C_2$ and $C_3{=}C_4$ bonds are characterized by two disynaptic attractors $V_{i=1,2}(C_1,C_2)$ and $V_{i=1,2}(C_3,C_4)$ of the point type lying approximately below and above the local symmetry plane. For the single C_2-C_3 bond, there is localized only one disynaptic attractor $V(C_2,C_3)$. We have to emphasize that in Figure 1, which shows a topology of the ELF function for the transition state, the $V_{i=1,2}(C_1,C_2)$ and $V_{i=1,2}(C_3,C_4)$ basins have been united to single basins $V(C_1,C_2)$ and $V(C_3,C_4)$. The basin population of $V_{1\cup2}(C_1,C_2)$ and $V_{1\cup2}(C_3,C_4)$ amounts to about 3.5 e, and that of $V(C_2,C_3)$ equals

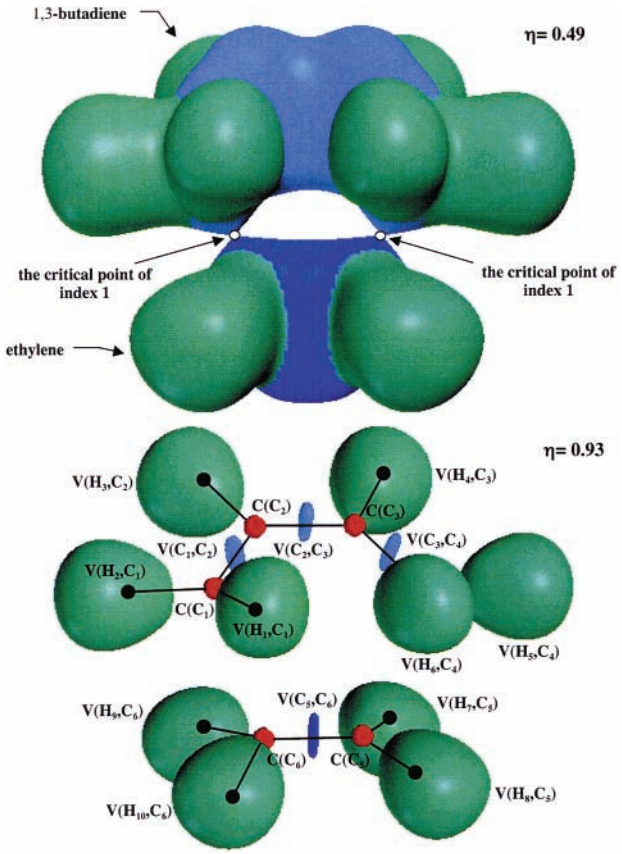

Figure 1. Localization basins in the transition state of a complex formed between ethylene and 1,3-butadiene in phase III of the reaction. The standard Lewis representation of bonding is superimposed on the ELF basins. Notice that the double bonds in both molecules are missing due to a union of pairs of basins: $V_{1,2}(C_1,C_2)$, $V_{1,2}(C_3,C_4)$, and $V_{1,2}(C_5,C_6)$ to single basins; $V(C_1,C_2)$, $V(C_3,C_4)$, and $V(C_5,C_6)$ observed in phases II and III.

2.23 e. One can notice that for the double bonds the populations are smaller than 4.0 e expected from a concept of two electron pairs formed in π-fashion and the electron density is moved to the single bond, which exhibits population larger than 2.0 e. Ethylene consists of two core basins $C(C_{i=5,6})$ with $\bar{N}$ of 2.06e, four protonated disynaptic basins $V(H_{j=7,10},C_{i=5,6})$ with populations of 2.10e, and two disynaptic basins $V_{i=1,2}(C_5,C_6)$ of the point type characterizing the double $C_5{=}C_6$ bond with the basin populations of 1.76e. In Figure 1, which represents TS in phase III, two $V_{i=1,2}(C_5,C_6)$ basins are united to singular basin $V(C_5,C_6)$.

In Figure 2, the reaction path calculated by means of the IRC method is shown, together with the Lewis representation of bonding for ethylene, 1,3-butadiene, and cyclohexadiene in all phases.

When the molecules begin to interact, as represented by the first point on the reaction path (R = 2.85Å), a topology of the ELF function is similar to those ones observed in isolated molecules. An analysis of the interaction region, between $C_1{\cdot}{\cdot}{\cdot}C_6$ and $C_4{\cdot}{\cdot}{\cdot}C_5$ atoms reveals two critical points of index 1 which are observed for gradient fields of $\rho(\mathbf{r})$ and $\eta(\mathbf{r})$. Further investigation shows singular critical point of index 2 localized approximately in the center of six-member ring of the C atoms. The number of localization basins in phase I equals 23, and it remains unchanged until first pair of catastrophes (R_C = 2.442Å). Phase I is one of the "longest" phases on the reaction path—in terms of nuclear displacement—as it lasts over 41 points (see Figure 2) and the total energy rises by 11.23 kcal/mol.

A comparison of the basin populations computed for different points on the reaction path (Table 1) presents that when 1,3-butadiene and ethylene approach the first bifurcations (R = 2.442 Å), a redistribution of the electron density in 1,3-butadiene is observed from the $V_{i=1,2}(C_1,C_2)$ and $V_{i=1,2}(C_3,C_4)$ basins to $V(C_2,C_3)$ and from $V_2(C_5,C_6)$ to $V_1(C_5,C_6)$ in ethylene. Thus, for the point preceding first pair of catastrophes (R = 2.45 Å), the basin population of the single bond in 1,3-butadiene increases to 2.41 e, and those of the double bonds decreases to 3.31 e. In ethylene a concentration of 1.76 is found for the electron density in the $V_1(C_5,C_6)$ basin with $\bar{N}$, larger than the 1.60 e found for $V_2(C_5,C_6)$. It is worth emphasizing that one could expect a flow of the electron density to the $V_2(C_5,C_6)$ basin—located out of six-member ring of C atoms—in order to minimize the Pauli repulsion as distances between basins decreases. However, the $V_1(C_5,C_6)$ basin is positioned closer

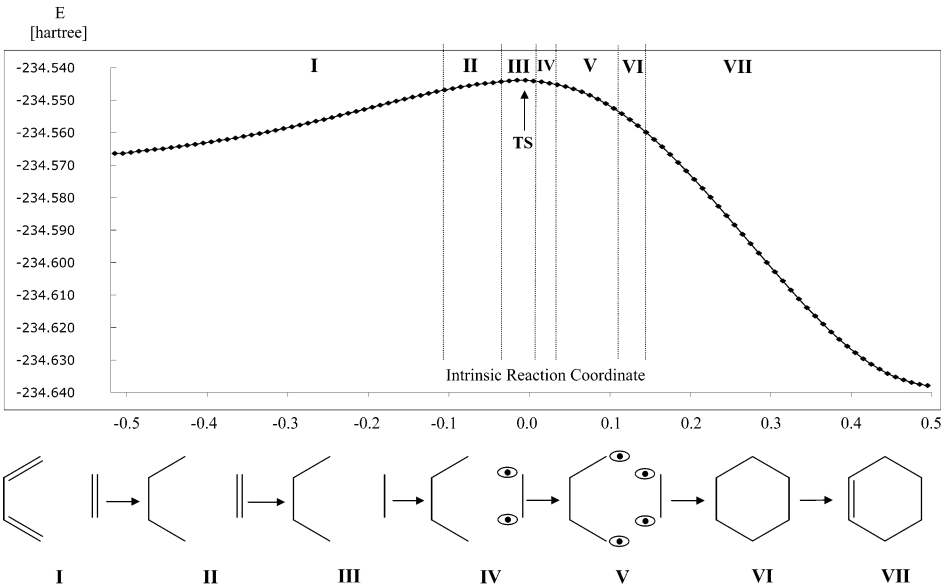

Figure 2. A fragment of the reaction path calculated by means of the IRC method for the reaction between ethylene and 1,3-butadiene. There are considered 102 points with step of 0.01 [amu$^{1/2}$bohr], and on the lateral axis the total energy [hartree] is shown. A bonding between atoms in all phases is demonstrated by the standard Lewis representation; however, in the case of phases IV and V, ellipses with points reflect the nonbonding electron density concentrated on the C atoms.

TABLE 1: The Basin Populations ($\bar{N}_i$) Calculated for the Localization Basins in the Ethylene−1,3-Butadiene Complex Corresponding to Different Points on the Reaction Path[a]

basin	phase I ethylene	phase I 1,3-butadiene	phase II $R_C = 2.442$Å	phase III $R = 2.316$ Å	phase IV $R = 2.229$ Å	phase V $R = 2.188$ Å	phase VI $R_C = 2.044$ Å	phase VII R = 1.984 Å	phase VII cyclohexadiene
$V_1(C_1,C_2)$	–	1.73	3.30	3.19	3.10	2.71	2.32	2.30	1.99
$V_2(C_1,C_2)$	–	1.73							
$V(C_1)$	–	–	–	–	–	0.34	–	–	–
$V_1(C_2,C_3)$	–	2.23	2.40	2.59	2.82	2.95	3.32	1.56	1.77
$V_2(C_2,C_3)$	–							1.84	1.81
$V_1(C_3,C_4)$	–	1.73	3.30	3.19	3.10	2.71	2.33	2.30	1.99
$V_2(C_3,C_4)$	–	1.73							
$V(C_4)$	–	–	–	–	–	0.34	–	–	–
$V(C_5)$	–	–	–	–	0.27	0.36	–	–	–
$V(C_4,C_5)$	–	–	–	–	–	–	1.18	1.22	1.84
$V(C_1,C_6)$	–	–	–	–	–	–	1.18	1.22	1.84
$V(C_6)$	–	–	–	–	0.27	0.36	–	–	
$V_1(C_5,C_6)$	1.76	–	1.78	3.32	2.80	2.64	2.27	2.23	1.89
$V_2(C_5,C_6)$	1.76	–	1.59						

[a] There are presented values for isolated molecules, points of catastrophes (R_C) and points localized in proximity of bifurcations (R). Only the valence $V(C_i,C_j)$ basins of the carbon−carbon bonds and nonbonding $V(C_i)$ basins are presented. The values of $\bar{N}_i$ are in [e]. In the case of the 1,3-butadiene molecule, the populations for the trans isomer are exhibited.

to the $C_1\cdots C_6$ and $C_4\cdots C_5$ interacting regions, and the increase of its population suggests that electron density will be concentrated between the C_1,C_6 and C_4,C_5 atoms in consecutive phases.

A comparison of the tree-reduction diagrams, which represent a reduction of localization domains in phase I (Figure 3), reveals that for $R \approx 2.55$Å there is an essential change in topology of the ELF function. When ethylene and 1,3-butadiene are placed at $R \geq 2.55$ Å, the first isolation for valence domains occurs for $\eta \approx 0.17$, leading to a separation of total valence domain surrounding the whole complex into molecular domains of ethylene and 1,3-butadiene. An isolation of basins of carbon cores in both molecules occurs at larger values of ELF. It implies that two weakly interacting molecules form the complex. This situation is changed when $R < 2.55$Å, as the core basins of carbon atoms are isolated before a splitting of total valence domain into the domains of ethylene and 1,3-butadiene. Therefore, from now the complex may be considered as "joined" by the electron density delocalized over ethylene and 1,3-butadiene. However, we have to emphasize that the C_4-C_5 and C_1-C_6 bonds have not been yet formally formed. The observed effect may be regarded as compatible with a ring current circulation along the molecular plane or in-plane aromaticity.[3,66−68]

The first pair of catastrophes occurs for $R_C = 2.442$ Å, and it determines phase II. Owing to the variation of the number (μ) of localization basins (morphic number) in each region of structural stability, these are typical miomorphic processes ($\Delta\mu < 0$) where the number of basins decreases from 23 to 21. In 1,3-butadiene two pairs of the disynaptic attractors—$V_{i=1,2}(C_1,C_2)$ and $V_{i=1,2}(C_3,C_4)$—and associated critical points of index 1 are annihilated, and new singulars attractors $V(C_1,C_2)$ and $V(C_3,C_4)$ are formed. Graphical representation of all critical points in this phase is shown in Figure 4a. Both catastrophes result in a loss of the double bond character for the $C_1{=}C_2$ and $C_3{=}C_4$ bonds, and from the classical (Lewis) point of view, all C−C bonds in 1,3-butadiene are now of the single bond type.

The local behavior of $\eta(\mathbf{r})$ in the neighborhood of the critical points is given, after translation to the origin and smooth change of variables by the unfolding: $\eta(x;u,v) = x^4 + ux^2 + vx$. This unfolding contains two control parameters (u,v) and one space variable (x). The space variable x is the direction of the eigenvector corresponding to the eigenvalue of the Hessian matrix which changes of sign, and the parameter u accounts for a separation between carbon atoms forming new bonds (is defined as $u = R_C - R$) and $v = 0$. These two catastrophes are cusps in Thom's classification.

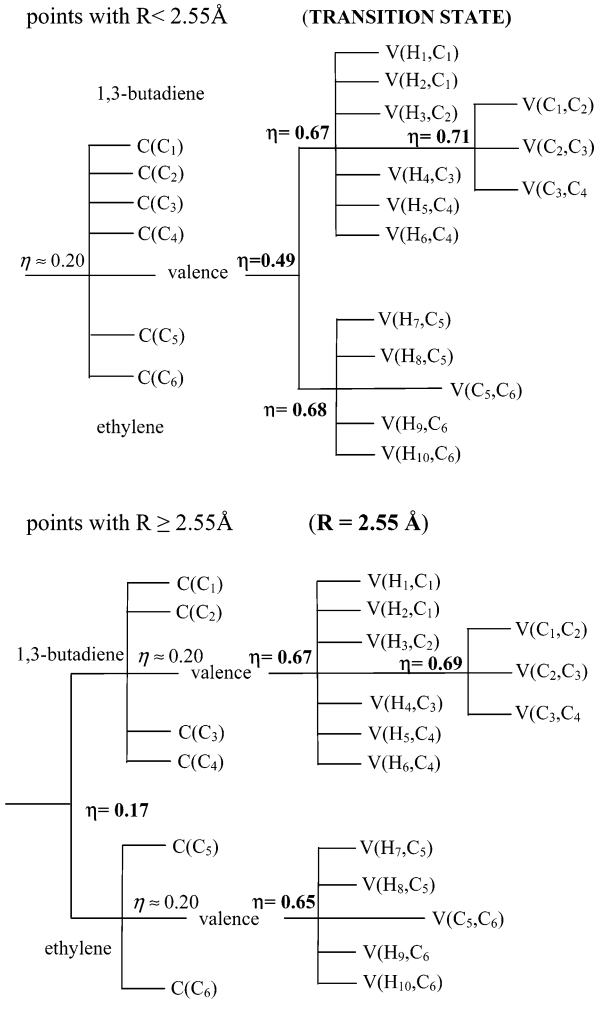

Figure 3. The tree-reduction diagrams obtained for the localization domains of the complex formed between ethylene and 1,3-butadiene. Two exemplary points are analyzed in phases I ($R = 2.55$Å) and III (TS). Owing to an order of first two bifurcations, i.e., (1) an isolation of molecular domains from a large domain surrounding whole complex and (2) an isolation of the core basins C(C), all points on the reaction path fall into two categories. For separations between ethylene and 1,3-butadiene where $R < 2.55$Å a topology of the ELF function resembles that one found for the transition state (phase III); meanwhile, for points with $R \geq 2.55$ Å; a topology is similar to that one obtained for $R = 2.55$Å. Abbreviations of basins correspond to those presented in Figure 1.

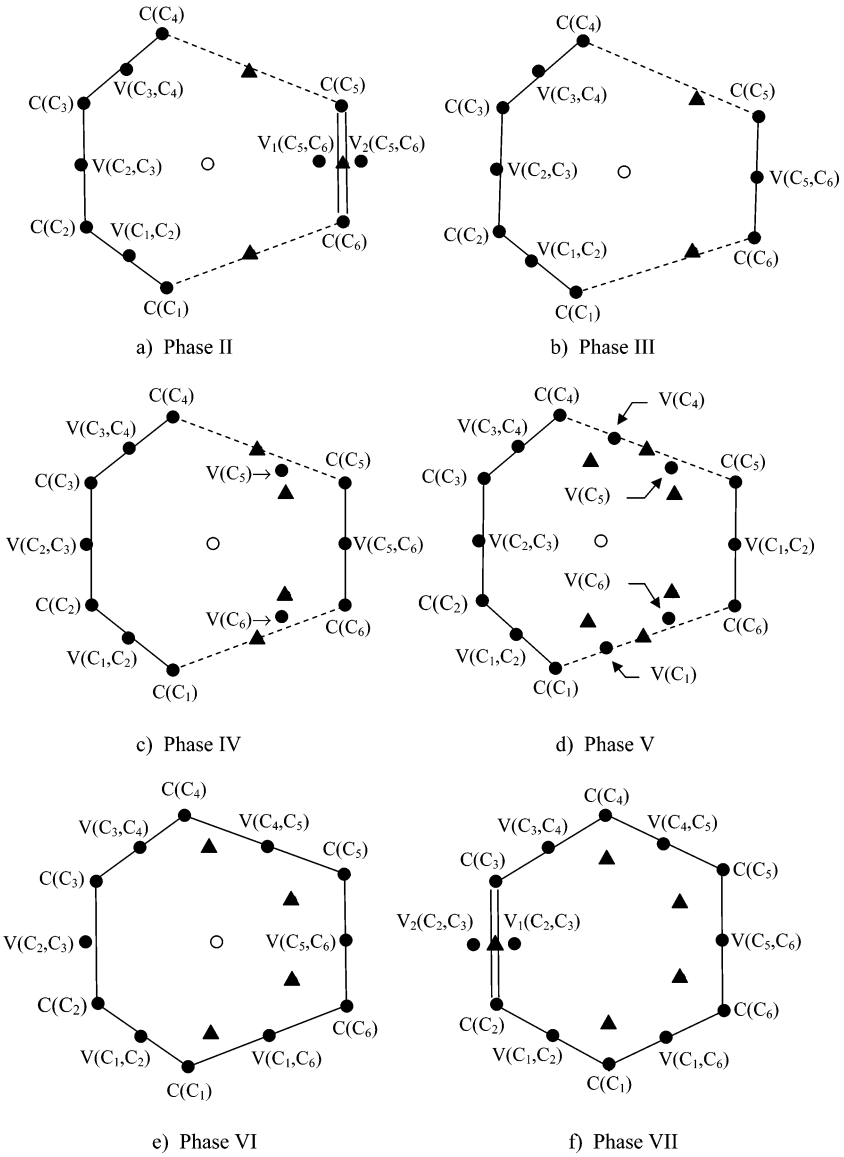

Figure 4. The critical points of index $I = 0$ (attractors) and 1 and 2 for phases from II to VII localized for the electron localization function (ELF) in the ethylene−1,3-butadiene complex. Hydrogen atoms are omitted for clarity, and only the critical points associated with investigated catastrophes are shown. For phase VII a structure corresponding to a minimum on the potential side is presented. Black circles, attractors; black triangles, critical points of index 1; empty circle, critical point of index 2. Solid lines correspond to the standard Lewis representation of bonding and dashed lines indicate an interaction between $C_{i=1,4;5,6}$ atoms forming new bonds.

Phase II is much "shorter" than stage I, and it runs only over seven points on the reaction path (Figure 2). An increase of the total energy by 1.47 kcal/mol is used for close up reacting molecules at intermolecular distances from about $R = 2.44$ to 2.32 Å followed by an intramolecular delocalization of the electron density over the 1,3-butadiene. A "reduction" of the double bonds to single bonds enables a much more effective delocalization of the electron density, which has begun in phase I. In the points of the catastrophes, an analysis of ethylene reveals the basin populations for $V_1(C_5,C_6)$ and $V_2(C_5,C_6)$ equal to 1.78 and 1.59 e, respectively presenting slightly larger polarization between basins than that found in phase I ($R =$ 2.45Å). For 1,3-butadiene, values of $\bar{N}$ for $V(C_1,C_2)$, $V(C_3,C_4)$, and $V(C_2,C_3)$ equal 3.30 and 2.40 e, respectively. Until the third catastrophe populations of $V(C_1,C_2)$, $V(C_3,C_4)$ decrease by about 0.1 e, and that of $V(C_2,C_3)$ rises by 0.19 e. In the case of the $C_5{=}C_6$ bond, their population slightly diminishes (by 0.05 e) in accordance to expected reduction of its double character in the next phase.

The third catastrophe, which occurs for $R_C \approx 2.32$ Å, characterizes the third phase of the reaction. It is similar to the previous pair of catastrophes and owing to Thom's classification belongs to the cusp type. In ethylene two disynaptic attractors $V_{i=1,2}(C_5,C_6)$ and an associated critical point of index 1 yield singular attractor $V(C_5,C_6)$. The graphical representation of critical points is shown in Figure 4b. The catastrophe characterizes a miomorphic process ($\Delta\mu < 0$), and the number of localization basins (μ) decreases from 21 to 22. From the classical (Lewis) point of view, phase III comprises all points on the reaction path where the double bonds in ethylene and 1,3-butadiene are "reduced" to the single bonds. As presented in Figure 2 it is relatively short and has been identified for 5 points on the reaction path with very small change of the total energy by only 0.12 kcal/mol.

It is worth to emphasize that phase III contains the transition state structure and there is not found any interesting event associated with TS. Additional information about the nature of bonding in the transition state may be deduced from the

representation of the localization basins in Figure 1 and the tree-reduction diagrams presented in Figure 3. A separation of the domain surrounding whole complex into domains of ethylene and 1,3-butadiene occurs at the index 1 saddle point for $\eta(\mathbf{r}) = 0.49$. It implies that the electron density in the $C_4\cdots C_5$ and $C_1\cdots C_6$ interacting regions or precisely around the saddle point corresponds to that of homogeneous electron gas and there is an absence of essential electron pairing. Moreover, one should notice that in a comparison with much smaller values of ELF ($\eta(\mathbf{r}) \approx 0.17$) found for the complex formed at larger intermolecular distances ($R > 2.55$ Å), the value of 0.49 may be interpreted as a reflection of large concentration of the electron density between interacting atoms.

After the catastrophe ($R = 2.316$Å), the basin populations of single $V(C_5,C_6)$ basin in ethylene equals 3.32 e, and for $V(C_1,C_2)$, $V(C_3,C_4)$, and $V(C_2,C_3)$, the populations of 3.19 and 2.59 e, respectively, have been calculated. During phase III ethylene and 1,3-butadiene are approached from 2.32 to 2.23 Å, and this change is followed by a redistribution of the electron density from $V(C_1,C_2)$ and $V(C_3,C_4)$ to $V(C_2,C_3)$ basin. An analysis of the basin populations calculated for a point preceding the second pair of catastrophes ($R = 2.243$Å) reveals a depletion of the $V(C_1,C_2)$ and $V(C_3,C_4)$ basins to 3.12 e and an increase of population of $V(C_2,C_3)$ to 2.76 e. It is important to note that in ethylene value of $\bar{N}$ for $V(C_5,C_6)$ is practically unaltered. A lack of change for $V(C_5,C_6)$ is easy to explain because new $V(C_5)$ and $V(C_6)$ basins are yet not formed; thus, the redistribution of the electron density theoretically would occur only (excluding participation of the C−H bonds and a change of the $V(C_5,C_6)$ volume) as an intermolecular transfer from ethylene to 1,3-butadiene. However, this is not favorable process, as confirmed by the qualitative relationship between a difference of the electrophilicity power for the dienophile/diene pair of DA reaction.[69] Both ethylene and 1,3-butadiene are classified as a marginal, and a moderate electrophile and nonpolar process associated with a pericyclic reaction is achieved. Furthermore, both have similar electronic chemical potential ($\mu = -0.1270$ and -0.1239 au, respectively); therefore, neither of them tends to provide charge to the other.[69]

The catastrophes four and five (the second pair of bifurcations), classified to the fold type, determine phase IV. They occur for $R_C \approx 2.23$ Å and lead to a formation in a neighborhood of the C_5 and C_6 atoms in ethylene single-point attractors $V(C_5)$ and $V(C_6)$ and associated with them critical points of index 1. These points lie on the gradient paths linking the $V(C_5)$ and $V(C_6)$ attractors with the $V(C_5,C_6)$ attractor. The new attractors belong to the monosynaptic type, and they reflect a concentration of the nonbonding electron density in the $C_4\cdots C_5$ and $C_1\cdots C_6$ regions. The graphical representation of attractors and other critical points associated with those catastrophes is presented in Figure 4c. The observed processes are plyomorphic ($\Delta\mu > 0$), and the number of localization basins increases from 20 to 22. The local behavior of the ELF function around the point of catastrophe is given by the unfolding: $\eta(x;\alpha) = x^3 + \alpha x$, where x is the direction of the eigenvector corresponding to the eigenvalue of the Hessian matrix which changes of sign and α parameter corresponds to a distance defined as $\alpha = R - R_C$.

It is interesting to put here a notion why the monosynaptic basins appear primarily on carbon atoms in ethylene. A close up of ethylene and 1,3-butadiene results in a mutual polarization between molecules reflected by enlarged Pauli repulsion among electrons. To compensate this effect and decrease the kinetic energy of electrons, a redistribution of the electron density is required. In 1,3-butadiene it is easy to realize because there is possible a flow of the electron density between basins: $V(C_1,C_2) \Rightarrow V(C_2,C_3) \Leftarrow V(C_3,C_4)$ from more populated (double bonds) to less populated (single bond). Actually this process is observed from a beginning of phase I. A similar response of a system is difficult to realize in ethylene where only one $V(C_5,C_6)$ basin and four protonated $V(H_{j=7,10},C_{i=5,6})$ basins largely saturated ($\bar{N} \approx 2.1$) are found. The electron density has to be "repelled" to new regions, and it is realized through a "creation" the $V(C_5)$ and $V(C_6)$ basins.

Phase IV is the "shortest" one because it lasts over only three points on the IRC path and it is associated with a change of the total energy by 0.82 kcal/mol. Furthermore, during this phase the $C_1\cdots C_6$ and $C_4\cdots C_5$ distances are shortened from 2.23 to 2.19Å. After the catastrophe ($R = 2.229$Å) the monosynaptic basins $V(C_5)$ and $V(C_6)$ exhibit the basin populations of 0.27 e, with very large value of the relative fluctuation 0.91 and the variance 0.24. It reveals that newly concentrated electron density is largely delocalized. A comparison of the populations between basins found in phase III and IV (Table 1) presents a transfer of the electron density from the C_1-C_2 and C_3-C_4 bonds to C_2-C_3 and from the C_5-C_6 bond to the $V(C_5)$ and $V(C_6)$ basins. At the point preceding third pair of catastrophes ($R = 2.20$ Å), the basin population of $V(C_1,C_2)$ and $V(C_3,C_4)$ is diminished to 3.05 e, and that of $V(C_2,C_3)$ increased by about 0.1 to 2.91 e. We have to emphasize that the C_1-C_2 and C_3-C_4 bonds possess still larger basin populations than C_2-C_3 and their inversion is expected to occur in the next phase. An analysis of ethylene reveals that the $V(C_5)$ and $V(C_6)$ basins are increased to 0.33 e after a redistribution of the electron density from $V(C_5,C_6)$ which the basin population is decreased from 2.80 to 2.69 e.

A further polarization of both molecules results in third pair of catastrophes (bifurcations 6 and 7), which characterizes phase V. They occur for $R_C \approx 2.19$ Å and correspond to a formation of two new attractors $V(C_1)$ and $V(C_4)$ and associated critical points of index 1. In the classification of Thom, they belong to the fold type and are analogous to those which appeared in phase IV. The attractors $V(C_1)$ and $V(C_4)$ are of the monosynaptic type, and they reflect a concentration of the nonbonding electron density around C_1 and C_4 atoms. The critical points of index 1 are located on the gradient paths linking $V(C_1)$ or $V(C_4)$ with $V(C_1,C_2)$ or $V(C_3,C_4)$ attractors, respectively. The observed catastrophes determine the plyomorphic processes because a number of localization basins increases from 22 to 24. A localization of critical points is presented in Figure 4d.

The appearance of the monosynaptic basins $V(C_1)$ and $V(C_4)$ which participate in a formation of new C_1-C_6 and C_4-C_5 bonds is a logical consequence of phase IV, where such basins were created on opposite side of "a sea" of the delocalized electron density, i.e., the C_5 and C_6 atoms in ethylene. Phase V is relatively "long" when compared to shorter phases: III, IV, or VI. In phase V, about seven points on the reaction path are presented, and they are associated with a decrease of the total energy by 8.86 kcal/mol. One can assume that "time" of this phase is needed to concentrate enough amount of the electron density in the interaction regions in order to overcome the Pauli repulsion among electrons coming from the $V(C_1)$, $V(C_4)$ and $V(C_5)$, $V(C_6)$ basins.

It is worth of mention that the observed mechanism of the reaction might be also explained in terms of a superposition of the resonance forms. The bonding in 1,3-butadiene can be represented by three Lewis structures: one entirely covalent

and two zwitterionic:

$$(+)H_2C-CH=CH-CH_2(-) \leftrightarrow H_2C=CH-CH=CH_2 \leftrightarrow (-)H_2C-CH=CH-CH_2(+)$$

Similar equilibrium can be proposed for ethylene:

$$(+)H_2C-CH_2(-) \leftrightarrow H_2C=CH_2 \leftrightarrow (-)H_2C-CH_2(+)$$

At the beginning of the reaction, when both molecules do not differ essentially from isolated states, the equilibriums are dominated by the covalent structures. A mutual polarization and a redistribution of the electron density occurring due the reaction course result in an increase of weights for the ionic forms. As a consequence, the formation of the monosynaptic basins $V(C_1)$, $V(C_4)$ and $V(C_5)$, $V(C_6)$ in phases IV and V reflect the concentration of the electron density on termini carbons.

After the catastrophes ($R = 2.188$Å) the newly created $V(C_1)$ and $V(C_4)$ basins exhibit the basin populations of 0.34 e, slightly smaller than $V(C_5)$ and $V(C_6)$ with 0.36 e. A comparison of the C_1-C_2, C_3-C_4, and C_2-C_3 bonds reveals an interesting effect. The population of $V(C_1,C_2)$ or $V(C_3,C_4)$—primarily corresponding to the double bonds—equals 2.71 e now, and it is smaller than that found for $V(C_2,C_3)$—at the beginning describing the single bond—with 2.95e. The electron density "contained" in the $V(C_1)$ and $V(C_4)$ basins is largely delocalized with the relative fluctuation of 0.89, and the variance equals 0.30. During phase V ethylene and 1,3-butadiene are approached from about 2.19 to 2.04 Å, and it is followed by a redistribution of the electron density from $V(C_1,C_2)$ and $V(C_3,C_4)$ to the monosynaptic basins: $V(C_1)$, $V(C_4)$ and $V(C_6)$, $V(C_5)$. Thus, for $R = 2.06$ Å (preceding catastrophes 8 and 9), a value of $\bar{N}$ for $V(C_1)$ and $V(C_4)$ increases to 0.62 e and that for $V(C_6)$ and $V(C_5)$ to 0.54 e. This alteration is obvious because a formation of new C_1-C_6 and C_4-C_5 bonds will occur in the next phase, and it requires a concentration of the electron density in the interaction region and enhancement of the electron pairing. Similarly, the population of the $V(C_2,C_3)$ basin rises from 2.95 to 3.31 e, revealing a continuous process of a formation of the double $C_2=C_3$ bond.

Phase VI constitutes—from the chemical point of view—the most important event on the reaction path. The fourth pair of catastrophes (bifurcations 8 and 9), which occurs at $R_C = 2.044$ Å, leads to a ring closure through a formation of new C_1-C_6 and C_4-C_5 bonds. In Thom's classification the catastrophes belong to the cusp type. Two pairs of monosynaptic attractors, i.e., $V(C_1)$, $V(C_4)$ and $V(C_5)$, $V(C_6)$, and respective critical points of index 1 are annihilated, and new disynaptic attractors $V(C_1,C_6)$ and $V(C_4,C_5)$ are created. The graphical representation of all critical points is shown in Figure 4e. The associated processes are of the miomorphic type ($\Delta\mu < 0$), and the number of basins decreases from 24 to 22.

An interpretation of the appearance of the $V(C_1,C_4)$ and $V(C_5,C_6)$ attractors on the basis of topological analysis of ELF is obvious: the covalent C_1-C_6 and C_4-C_5 bonds between ethylene and 1,3-butadiene have been formed. However, one has to be conscious that their attractor's basins are not yet entirely "filled" with the electron density and respective "formation" process is terminated in phase VII. Furthermore, it is worth to emphasize that for the first time, we are able to show exactly a distance at which new bonds are formed, i.e., $R = 2.044$Å. A dissociation of new C_1-C_6 and C_4-C_5 bonds into two pair of monosynaptic attractors $V(C_i)$—interpreted on the basis of the BET[32]—yields proof that they belong to the covalent polarized type.

Phase VI is short, as it has been identified only for four points on the reaction path with a decrease of the total energy by 1.30 kcal/mol. An analysis of populations shows that after the formation of the $V(C_1,C_6)$ and $V(C_4,C_5)$ basins, their values of $\bar{N}$ amount to 1.18 e, with a variance of 0.81. As revealed by a comparison of data presented in Table 1 during phase VI, the electron density is redistributed from $V(C_5,C_6)$ to newly formed $V(C_1,C_6)$ and $V(C_4,C_5)$ basins and from $V(C_1,C_2)$ and $V(C_3,C_4)$ to $V(C_2,C_3)$. The latter process, i.e., a concentration of the electron density in a space between the C_2 and C_3 atoms, is required in order to form the $C_2=C_3$ double bond.

The last (VII) phase on the reaction path is determined by tenth catastrophe, and it comprises slightly smaller number of points on the reaction path (35) than that found for phase I. The catastrophe results in a formation the double $C_2=C_3$ bond in (former) 1,3-butadiene molecule. It occurs for $R_C \approx 1.98$Å ,and the disynaptic $V(C_2,C_3)$ attractor yields two $V_{i=1,2}(C_2,C_3)$ attractors and the critical point of index 1. Due to the Thom's classification, this catastrophe belongs to the cusp type, and the observed process is a polymorphic one, as the number of localization basins increases from 22 to 23. A graphical representation of the critical points is presented in Figure 4f. One can notice that this catastrophe is similar to those ones leading from phase I to II or II to III, where the double C=C bonds have been decayed.

The reaction and phase VII is terminated for the cyclohexadiene molecule, which corresponds to the minimum on the product. The respective bond lengths have been finally obtained: C_1-C_2, C_3-C_4, 1.509 Å; C_2-C_3, 1.337 Å; C_4-C_5 and C_1-C_6, 1.549 Å; C_5-C_6, 1.554 Å. During this phase the total energy decreases by 43.1 kcal/mol, and it is associated with a redistribution of the electron density from the C_1-C_2, C_3-C_4, and C_5-C_6 single bonds to the newly formed double $C_2=C_3$ bond and the "intermolecular" C_4-C_5 and C_1-C_6 bonds. After the catastrophe ($R = 1.984$ Å) the basin population of the $V_1(C_2,C_3)$ and $V_2(C_2,C_3)$ basins equals 1.56 and 1.84 e, respectively. At the final point, the cyclohexadiene molecule, the value of $\bar{N}$ for $V_2(C_2,C_3)$, is slightly diminished to 1.81 e, and that of $V_1(C_2,C_3)$ is increased by about 0.2 e to 1.77 e. A sum of the populations for $V_1(C_2,C_3)$ and $V_2(C_2,C_3)$ yields the bond order of 1.8, which is close to the 2.0 expected on the basis of the standard Lewis representation for the double bond. A value of $\bar{N}$ for $V(C_1,C_2)$ and $V(C_3,C_4)$ equal to 2.30e is eventually diminished to 1.99 e, which confirms the observation that the electron density flows from single to double bonds. Similarly, the basin population of $V(C_5,C_6)$ of 2.23 e is reduced to 1.89 e, and this alteration may be associated with an increase of $\bar{N}$ for $V(C_1,C_6)$ and $V(C_4,C_5)$ with 1.22−1.84 e found after the catastrophe.

4.2. A Comparison to a Valence Bond Approach. Due to a suggestion done by one of referees, it is worth examining the work of Shaik,[70] who adopted a valence bond approach in order to answer to a question: "What happens to molecules as they react?" He suggested that in all reactions which involve covalent bond-making and bond-breaking steps, there is a preparation of the reactants for bonding via a transformation to open shell entities in order to create new bonds and break old ones. Therefore, for the reaction between ethylene and 1,3-butadiene, one would expect that one of the reactants may be in the excited triplet state and the second one in the ground singlet state. The analysis of the ELF function shows that a preparation for bonding is achieved by a concentration of the electron density in the nonbonding $V(C_5)$, $V(C_6)$ and $V(C_1)$, $V(C_4)$ basins but the interacting system is described by the singlet state. To find

TABLE 2: A Comparison of the Basin Populations ($\bar{N}_i$) Calculated for the Ethylene−1,3-Butadiene Complex and Isolated Molecules in the Singlet and Triplet Electronic States[a]

	phase IV ($R = 2.199$Å)				phase V ($R = 2.056$Å)			
basin	molecules (triplet)	molecules (singlet)	complex (triplet)	complex (singlet)	molecules (triplet)	molecules (singlet)	complex (triplet)	complex (singlet)
	1,3-Butadiene				1,3-Butadiene			
$V_1(C_1,C_2)$	} 2.34 (0.10)	} 3.39	} 2.51 (0.06)	} 3.05	} 2.25 (0.08)	} 3.33	} 2.81 (0.16)	} 2.34
$V_2(C_1,C_2)$								
$V(C_1)$	0.51 (0.13)	−	0.76 (0.06)	−	0.64 (0.16)	−	0.51 (−0.01)	0.62
$V_1(C_2,C_3)$	} 3.21 (0.11)	} 2.35	} 2.74 (0.15)	} 2.91	} 3.27 (0.08)	} 2.43	} 2.22 (0.13)	} 3.31
$V_2(C_2,C_3)$								
$V_1(C_3,C_4)$	} 2.34 (0.10)	} 3.37	} 2.50 (0.06)	} 3.05	} 2.25 (0.08)	} 3.33	} 2.81 (0.16)	} 2.34
$V_2(C_3,C_4)$								
$V(C_4)$	0.51 (0.13)	−	0.76 (0.06)	−	0.64 (0.16)	−	0.51 (−0.01)	0.62
	Ethylene				Ethylene			
$V(C_5)$	0.62 (0.19)	−	−	0.34	0.73 (0.22)	−	0.70 (0.07)	0.54
$V(C_6)$	0.62 (0.19)	−	−	0.34	0.73 (0.22)	−	0.70 (0.07)	0.54
$V_1(C_5,C_6)$	} 2.07 (0.14)	1.68	} 2.84 (0.16)	} 2.69	} 1.98 (0.13)	} 3.38	} 2.10 (0.06)	} 2.28
$V_2(C_5,C_6)$		1.77						

[a] Two points are investigated for $R = 2.199$ Å (phase IV) and $R = 2.056$ Å (phase V). Only the valence $V(C_i,C_j)$ basins of the carbon−carbon bonds and nonbonding $V(C_i)$ basins are presented. The values of $\bar{N}_i$ are in [e] and in parentheses the integrated basin spin density $\langle S_Z \rangle$ is shown, which is defined as $\langle S_Z \rangle_{\Omega i} = 1/2 \int_{\Omega i} (\rho^{\alpha}(\mathbf{r}) - \rho^{\beta}(\mathbf{r}))\, d\mathbf{r}$. In all cases optimized geometries in the singlet state from the IRC calculations have been used.

a support for the concept of Shaik,[70] we decided to compare a topology of the ELF function of isolated ethylene and 1,3-butadiene computed in the singlet and triplet states with those ones in the complex described by the singlet electronic state. This methodology is very simplified, but it seems to be the only possibility when one uses the single configurational approximation of the wave function based on the DFT method. In Table 2 there are presented results of calculations for two points in phases IV and V for distances $R = 2.199$ and 2.056 Å, respectively. A comparison of topology of the ELF function presents that for $R = 2.199$ Å the 1,3-butadiene molecule in the triplet state differs essentially from its counterpart in the complex (singlet). There are found two nonbonding basins $V(C_1)$ and $V(C_4)$ which are not observed in the complex. Furthermore, the basin population shows a larger concentration of the electron density in the C_2-C_3 bond (3.21 e) than in C_1-C_2 and C_3-C_4 (2.34 e), in contrary to values found for the complex where the larger values of $\bar{N}$ are computed for the C_1-C_2 and C_3-C_4 bonds. In the case of ethylene, there is not any difference in topology of the ELF function between isolated case (triplet) and the complex; however, one can observe a much larger concentration of the electron density in the $V(C_5)$ and $V(C_6)$ basins (0.62 e) than obtained for the complex (0.34 e).

As one could expect, the largest differences appear for the complex calculated in the triplet electronic state. The ethylene molecule is characterized by only one $V(C_5,C_6)$ basin, and an absence of $V(C_5)$ and $V(C_6)$ reflects that we are on the repulsive part of PES. For 1,3-butadiene one can observe the $V(C_1)$ and $V(C_4)$ basins—which are not present in the complex (singlet)—with larger populations (0.76 e) than found in the isolated case (triplet).

A much interesting conclusions are obtained for the second investigated point ($R = 2.056$Å), which describes a situation in proximity of the catastrophes 8 and 9, leading to the ring closure. To our surprise, a topology of the ELF function of 1,3-butadiene (triplet) is very similar to that one in the complex (singlet), and differences of the basin populations computed for $V(C_1)$, $V(C_4)$ and $V(C_1,C_2)$, $V(C_3,C_4)$ and $V(C_2,C_3)$ equal 0.02, 0.1, and 0.05 e, respectively. It suggests that the proposal of Shaik may be true and 1,3-butadiene exists in the complex in the triplet electronic state—at least in proximity of bifurcations. An analysis of 1,3-butadiene in the singlet state supports that conclusion because its topology of the ELF function differs essentially from that one found for the complex and for instance there are not found the nonbonding $V(C_1)$ and $V(C_4)$ basins.

In the complex calculated in the triplet state, one can notice much better resemblance of the complex in the singlet state found for $R = 2.056$ Å than for $R = 2.199$ Å. A topology of the ELF function of 1,3-butadiene and ethylene reveals the same attractors in both electronic states. Furthermore, the integrated spin density of the $V(C_1)$ and $V(C_4)$ basins presents slightly larger values of the beta electron density (−0.01e), which would suggest a preparation for a pairing with alpha electrons concentrated on nonbonding basins in ethylene. An analysis of 1,3-butadiene in the singlet state shows that its picture of electron localization does not resemble a situation of the complex because of absence of the monosynaptic $V(C_1)$ and $V(C_4)$ basins.

If we assume, on the basis of our very simplified results, that the electronic state of 1,3-butadiene might be characterized as the triplet state, it is rather impossible to draw an analogous conclusion in the case of ethylene, whose electronic state should correspond to singlet. For both investigated points, the ELF function calculated for the singlet state of ethylene differs essentially from that one observed in the complex. For intermolecular distance $R = 2.199$ Å, the $C_5{=}C_6$ bond is described by two bonding basins $V_1(C_5,C_6)$ and $V_2(C_5,C_6)$, and the $V(C_5)$ and $V(C_6)$ basins are missing. The achieved picture corresponds to phases I and II of the reaction before a reduction of the double to single bonds. In the case of point at $R = 2.056$ Å, there is found only one $V(C_5,C_6)$ basin—after a reduction to the single bond—but its basin population of 3.38 e is about 1 e larger than that in the complex and it is caused by an absence of the monosynaptic basins.

On the basis of obtained results, it is obvious that description of isolated ethylene in the singlet state as a model of its electronic state in the complex leads to rather poor conclusions. One could even find that the triplet state is better description of ethylene in the complex because of presence of the $V(C_5)$ and $V(C_6)$ basins (for both points) which are absent in the singlet calculations. Furthermore, the large discrepancy between the singlet state of isolated ethylene and its counterpart in the complex can be explained by two factors: (1) in the complex there is present large electrostatic interaction between the

reactants which leads to additional redistribution of the electron density reflected by monosynaptic basins $V(C_5)$ and $V(C_6)$; (2) the electronic state of ethylene in the complex cannot be considered as "pure" singlet state even using the multicofigurational CI method, and it can be described as "prepared" for the reaction via a not negligible contribution of the triple state to the wave function.

5. Conclusions

The catastrophe theory has been used to investigate the reorganization of the localization basins, within the ELF formalism, along the reaction path between 1,3-butadiene and ethylene. The reaction consists of seven phases characterized by 10 catastrophes, within of the classification given by René Thom, belonging to the fold and cusp types. All catastrophes occur at the intermolecular distances $R(C_1\cdots C_6)$ and $R(C_4\cdots C_5)$ ranging between 2.44 and 1.98 Å.

At the first state of the reaction the interaction between both molecules produces a redistribution of the electron density on 1,3-butadiene and ethylene that is achieved by a "reduction" of the $C_1{=}C_2$, $C_3{=}C_4$ and $C_5{=}C_6$ double bonds to single bonds. In the course of the reaction, an effect of mutual polarization between the reacting molecules is observed. First, two basins, $V(C_5)$ and $V(C_6)$, are created at ethylene. In the case of 1,3-butadiene, the formation of the $C_2{-}C_3$ double bond compensates the effect of polarization. The formation of the $C_1{-}C_6$ and $C_4{-}C_5$ bonds is preceded by concentrations of the nonbonding electron density on the termini C_1, C_4, C_5, and C_6 atoms, as revealed by respective monosynaptic basins.

The TS found on PES does not correspond to any change of structural stability of the ELF function but relatively large value of $\eta(\mathbf{r}) = 0.49$ is found for the critical point of index 1 in the $C_1\cdots C_6$ and $C_4\cdots C_5$ regions. From the topological view on the ELF function in the reacting complex, the formation of new $C_1{-}C_6$ and $C_4{-}C_5$ bonds between 1,3-butadiene and ethylene occurs at $R = 2.044$ Å as a consequence of two cusp catastrophes.

Acknowledgment. S.B. would like to thank professor Juan Andrés for his kind hospitality during stay at University of Jaume I. The "Wroclaw Centre for Networking and Supercomputing", where a part of the computations has been performed, is thanked for the granted time. The Marie Curie Development Host Fellowship program supported the work of S.B.—contract N° HPMD-CT-2000-00055. (The authors are solely responsible for the information communicated, and it does not represent the opinion of The European Community. The European Community is not responsible for any use that might be made of data appearing therein.) J.A. acknowledges financial support from Universitat Jaume I-Fundacio Bancaixa, Project P1B99-02.

References and Notes

(1) Fradera, X.; Austen, M. A.; Bader, R. F. W. *J. Phys. Chem. A* **1999**, *103*, 304.
(2) Poater, J.; Solà, M.; Duran, M.; Fradera, X. *J. Phys. Chem. A* **2001**, *105*, 6249.
(3) Poater, J.; Solà, M.; Duran, M.; Fradera, X. *J. Phys. Chem. A* **2001**, *105*, 2052; Erratum. *J. Phys. Chem. A* **2002**, *106*, 4794.
(4) Bader, R. F. *Atoms in Molecules: A Quantum Theory*; Oxford University Press: Oxford, 1994.
(5) Becke, A. D.; Edgecombe, K. E. *J. Chem. Phys*. **1990**, *92*, 5397.
(6) Silvi, B.; Savin, A. *Nature* **1994**, *371*, 683.
(7) Savin, A.; Becke, A. D.; Flad, J.; Nesper, R.; Preuss, H.; von Schnering, H. G. *Angew. Chem., Int. Ed. Engl*. **1991**, *30*, 409.
(8) Savin, A.; Silvi, B.; Colonna, F. *Can J. Chem*. **1996**, *74*, 1088.
(9) Kohout, M.; Savin, A. *Int. J. Quantum Chem*. **1996**, *60*, 875.
(10) Savin, A.; Nesper, R.; Wengert, S.; Fässler, T. *Angew. Chem., Int. Ed. Engl*. **1997**, *36*, 1809.
(11) Marx, D.; Savin, A. *Angew. Chem., Int. Ed. Engl*. **1997**, *36*, 2077.
(12) Noury, S.; Colonna, F.; Savin, A.; Silvi, B. *J. Mol. Struct*. **1998**, *450*, 59.
(13) McWeeny, R. *Rev. Mod. Phys*. **1960**, *32*, 335.
(14) McWeeny, R. *Methods of Molecular Quantum Mechanics*, 2nd ed.; Academic Press: New York, 1989.
(15) Chamorro, E.; Santos, J. C.; Gómez, B.; Contreras R.; Fuentealba, P. *J. Phys. Chem. A.* **2002**, *106*, 11533.
(16) Chamorro, E.; Toro-Labbé, A.; Fuentealba, P. *J. Phys. Chem. A* **2002**, *106*, 3891.
(17) Oliva, M.; Safont, V. S.; Andrés, J.; Tapia, O. *Chem. Phys. Lett.* **2001**, *340*, 391.
(18) Silvi, B.; Savin, A.; Wagner, F. R. In *Modelling of Minerals and Silicated Materials*; Topics in Molecular Organization and Engineering Edition; Silvi, B.; D'Arco, P., Eds.; Kluwer Academic Publishers: Dordrecht, The Netherlands, 1997; Vol. 15, pp 179−199.
(19) Llusar, R.; Beltrán, A.; Andrés, J. Noury, S.; Silvi, B. *J. Comput. Chem*. **1999**, *20*, 1517.
(20) Beltrán, A.; Andrés, J.; Noury, S.; Silvi, B. *J. Phys. Chem. A* **1999**, *103*, 3078.
(21) Fuster, F.; Silvi, B. *Theor. Chem. Acc*. **2000**, *104*, 13.
(22) Silvi, B.; Gatti, C. *J. Phys. Chem. A* **2000**, *104*, 947.
(23) Choukroun, R.; Donnadieu, B.; Zhao, J.-S.; Cassoux, P.; Lepetit, C.; Silvi, B. *Organometallics* **2000**, *19*, 1901.
(24) Chestnut, D. B.; Bartolotti, L. *J. Chem. Phys*. **2000**, *253*, 1.
(25) Chestnut, D. B.; Bartolotti, L. *J. Chem. Phys*. **2000**, *257*, 171.
(26) Fressigné, C.; Maddaluno, J.; Marquez, A.; Giessner-Prettre, C. *J. Org. Chem*. **2001**, *65*, 8899.
(27) Boily, J. *J. Phys. Chem. A* **2002**, *106*, 4718.
(28) Häussermann, U.; Wengert, S.; Nesper, R. *Angew. Chem., Int. Ed. Engl*. **1994**, *33*, 2073.
(29) Chamorro, E.; Santos, J. C.; Gómez, B.; Contreras, R.; Fuentealba, P. *J. Chem. Phys.* **2001**, *114*, 23.
(30) Poston, T.; Stewart I. *Catastrophe Theory and Its Applications*; Dover Publications: Mineola, NY, 1996.
(31) Thom, R. *Stabilité Structurelle et Morphogénèse*; Intereditions: Paris, 1972.
(32) Krokidis, X.; Noury, S.; Silvi, B. *J. Phys. Chem. A*. **1997**, *101*, 7277.
(33) Krokidis, X.; Goncalves, V.; Savin, B. *J. Phys. Chem. A* **1998**, *102*, 5065.
(34) Krokidis, X.; Vuilleumier, R.; Borgis, D.; Silvi, B. *Mol. Phys*. **1999**, *96*, 265.
(35) Krokidis, X.; Silvi, B.; Sevin, A. *New J. Chem*. **1998**, *22*, 1341.
(36) Krokidis, X.; Silvi, B.; Alikhani, M. E. *Chem. Phys. Lett*. **1988**, *292*, 35.
(37) Michelini, M. C.; Sicilia, E.; Russo, N.; Alikhani, M. E.; Silvi, B. *J. Phys. Chem. A*, submitted.
(38) Finguelli, F.; Tatichi, A. *The Diels-Alder Reaction. Selected Paractical Methods*; Wiley: New York, **2002**.
(39) Evans, M. G. *Trans. Faraday Soc.* **1939**, *35*, 824.
(40) Carruthers, W. *Some Modern Methods of Organic Synthesis*, 2nd ed.; Cambridge University Press: Cambridge, 1978.
(41) Carruthers, W. *Cycloaddition Reactions in Organic Synthesis*; Pergamon: Oxford, 1990.
(42) Diels, O.; Alder, K. *Justus Liebigs Ann. Chem*. **1928**, *460*, 98.
(43) Woodward, R. B.; Hoffmann, R. *Angew. Chem., Int. Ed. Engl.* **1969**, *8*, 781.
(44) Sauer, J. *Angew. Chem. Int., Ed. Engl*. **1966**, *5*, 211.
(45) Sauer, J. *Angew. Chem. Int., Ed. Engl*. **1967**, *6*, 16.
(46) Dewar, M. J. S.; Olivella, S.; Stewart, J. J. P. *J. Am. Chem. Soc*. **1986**, *108*, 5771.
(47) (a) Wiest, O.; Montiel, D. C.; Houk, K. N. *J. Phys. Chem. A* **1997**, *101*, 8378. (b) Houk, K. N.; Beno, B. R.; Nendel, M.; Black, K.; Yoo, H. Y.; Wilsey, S.; Lee, J. K. *THEOCHEM* **1997**, *398*−*399*, 169. (c) Hrovat, D. A.; Beno, B. R.; Lange, H.; Yoo, H.-Y.; Houk, K. N.; Borden, W. T. *J. Am. Chem. Soc*. **2000**, *122*, 7456. (d) Houk, K. N.; González, J.; Li, Y. *Acc. Chem. Res*. **1995**, *28*, 81.
(48) Diau, E. W.-G.; De Feyter, S.; Zewail, A. H. *Chem. Phys. Lett*. **1999**, *304*, 134.
(49) Sakai, S. *J. Phys. Chem. A* **2000**, *104*, 922.
(50) Lewis, G. N. *J. Am. Chem. Soc*. **1916**, *38*, 762.
(51) Lewis, G. N. *Valence and the Structure of Atoms and Molecules*; Dover: New York, 1966.
(52) Silvi, B. *J. Phys. Chem. A* **2003**, *107*, 3081.
(53) Dobson, J. F. *J. Chem. Phys.* **1991**, *94*, 4328.
(54) Mezey, P. G. *Can. J. Chem*. **1993**, *72*, 928.
(55) Tal, Y.; Bader, R. F. W.; Nguyen-Dang, T. T.; Ojha, M.; Anderson, S. G. *J. Chem. Phys.* **1981**, *74*, 5162.
(56) Bader, R. F. W.; Nguyen-Dang, T. T.; Tal, Y. *Rep. Prog. Phys*. **1981**, *44*, 893.

(57) Cioslowski, J. *J. Phys. Chem*. **1990**, *94*, 5496.
(58) Becke, A. D. *J. Chem. Phys.* **1993**, *98*, 1372.
(59) Becke, A. D. *J. Chem. Phys.* **1993**, *98*, 5648.
(60) Lee, C.; Yang, W.; Parr, R. G. *Phys. Rev. B* **1988**, *37*, 785.
(61) Frisch, M. J.; Trucks, G. W.; Schlegel, H. B.; Scuseria, G. E.; Robb, M. A.; Cheeseman, J. R.; Zakrzewski, V. G.; Montgomery, J. A.; Stratmann, Jr., R. E.; Burant, J. C.; Dapprich, S.; Millam, J. M.; Daniels, A. D.; Kudin, K. N.; Strain, M. C.; Farkas, O.; Tomasi, J.; Barone, V.; Cossi, M.; Cammi, R.; Mennucci, B.; Pomelli, C.; Adamo, C.; Clifford, S.; Ochterski, J.; Petersson, G. A.; Ayala, P. Y.; Cui, Q.; Morokuma, K.; Malick, D. K.; Rabuck, A. D.; Raghavachari, K.; Foresman, J. B.; Cioslowski, J.; Ortiz, J. V.; Baboul, A. G.; Stefanov, B. B.; Liu, G.; Liashenko, A.; Piskorz, P.; Komaromi, I.; Gomperts, R.; Martin, R. L.; Fox, D. J.; Keith, T.; Al-Laham, M. A.; Peng, C. Y.; Nanayakkara, A.; Challacombe, M.; Gill, P. M. W.; Johnson, B.; Chen, W.; Wong, M. W.; Andres, J. L.; Gonzalez, C.; Head-Gordon, M.; Replogle, E. S.; Pople, J. A. *Gaussian 98*, Revision A.9; Gaussian, Inc.: Pittsburgh, PA, 1998.
(62) Fukui, K. *J. Phys. Chem*. **1970**, *74*, 4161.
(63) Gonzalez, C.; Schlegel, H. B. *J. Phys. Chem*. **1990**, *94*, 5223.
(64) Noury, S.; Krokidis, X.; Fuster, F.; Silvi, B. *Comp&Chem*. **1999**, *23*, 597.
(65) Pepke, E.; Murray, J.; Lyons, J.; Hwu, T.-Z. *SciaAn*; Supercomputer Computations Research Institute: Tallahassee, FL, 1993.
(66) Herges, R.; Jiao, H.; Schleyer, P. v. R. *Angew. Chem., Int. Ed. Eng*. **1994**, *33*, 1376.
(67) Jiao, H.; Schleyer, P. v. R. *J. Phys. Org. Chem*. **1998**, *11*, 655.
(68) Cheng, M.-F.; Li, W.-K. *Chem. Phys. Lett*. **2003**, *368*, 630.
(69) Domingo, L. R.; Aurell, M. J.; Pérez, P.; Contreras, R. *Tetrahedron* **2002**, *58*, 4417.
(70) Shaik, S. S., *J. Am. Chem. Soc*. **1981**, *103*, 3692.